



The physics of frost heave and ice-lens growth

by

**Stephen S. L. Peppin
Robert W. Style**

The physics of frost heave and ice-lens growth

Stephen S. L. Peppin¹ Robert W. Style²

April 16, 2012

¹Oxford Centre for Collaborative Applied Mathematics, University of Oxford,
Mathematical Institute, 24-29 St. Giles', Oxford, OX1 3LB, UK

²Department of Geology & Geophysics, Yale University, New Haven, CT, 06520-8109,
USA

Abstract

The formation of rhythmic lenses of ice in freezing soils is an intriguing geophysical phenomenon that is not fully understood, despite much experimental and theoretical work over the past century. We review proposed mathematical models of ice lens growth and frost heave, from early capillary theories and models based on the concept of a frozen fringe, to more recent advances that have revitalised the capillary model. In addition we identify several key experimental and theoretical challenges that are still to be resolved.

1 Introduction

Frost heave refers to the upward displacement of the ground surface caused by the formation of ice lenses – discrete bands of ice that form in freezing soil. This phenomenon is partly responsible for beautiful surface patterns that appear in very cold, permafrost areas (figure 1). Similar patterned ground has been observed on ice-rich portions of Mars, and the observations have been used to draw interesting conclusions about previous climate conditions [1]. Frost heave also has many practical and industrial implications. Residents in cold countries are familiar with the annual appearance of frost-heave-induced road damage after winter cold spells, and the heaving forces are capable of damaging



Figure 1: Phenomena caused by frost heave. Clockwise from top left: a pipeline heaved out of the ground [3], hummocks, stone circles and road buckling [2].

25 infrastructure such as pipelines, railways and buildings (figure 1). In the United States,
26 over two billion dollars is spent annually repairing frost-heave damage to roads alone [2].
27 Thus worldwide, the cost is tremendous.

28 Despite the importance of frost heave, there are still many unanswered questions
29 about the underlying mechanisms. Almost a century has passed since Stephen Taber
30 demonstrated experimentally the basic features of frost heave [4, 5, 6], and scientists are
31 still actively working to understand his observations. Taber’s key result was that frost
32 heave is not, as commonly assumed, caused by the expansion of water upon freezing; he
33 showed that a column of soil saturated with benzene (a liquid that contracts as it freezes)
34 also experiences frost heave. Instead Taber demonstrated that frost heave is caused by
35 the migration of water from lower, unfrozen regions of a soil column towards the freezing
36 front. There, it deposits as bands of pure ice in the soil – ice lenses – which force the
37 soil apart as they grow, heaving the surface upwards. This process can cause almost
38 unlimited heave of the soil surface, provided there is a sufficient supply of water and slow
39 enough freezing [5, 6, 7].

40 Any quantitative theory of frost heave must explain two salient features of the phe-

41 nomenon: the migration of water from lower, unfrozen regions of the soil to colder regions
 42 where it freezes as excess ice, and the tendency of the ice to force the soil apart and de-
 43 posit as periodic ice lenses. In this work we review the various mathematical models that
 44 have been proposed since the 1930s. We classify the theories into two broad categories,
 45 capillary models and frozen-fringe models, choosing representative works for each, rather
 46 than attempting an exhaustive list of all published theories.

47 2 Capillary theory

48 2.1 Suction of water towards the ice lens

49 The first widely accepted explanation for frost heave was given by Taber [6] and later
 50 quantified by Beskow [7], Gold [8], Jackson et al. [9, 10] and Everett [11]. This theory
 51 relies on the Clapeyron equation describing thermodynamic equilibrium in a system at
 52 temperature T and containing ice at pressure P_i and water at P_w [12, 9, 13]:

$$P_i - P_w = \frac{\rho_w L_f}{T_m} (T_m - T). \quad (1)$$

53 Here L_f is the latent heat of fusion at the bulk freezing temperature T_m and atmospheric
 54 pressure P_{atm} , and ρ_w is the density of water. In fact this is not the complete version of
 55 the Clapeyron equation, as equation (1) neglects a term $(\rho_w/\rho_i - 1)(P_{atm} - P_i)$, where ρ_i
 56 is the density of ice [11]. This term is typically small since $\rho_w \approx \rho_i$.

57 Figure 2(a) shows a simple system that illustrates the basic frost heave phenomenon
 58 [9]. There is a layer of ice above a water-saturated soil, which in turn sits on a reservoir
 59 containing water at pressure P_R . The whole system is isothermal with temperature
 60 $T < T_m$. The pore water and reservoir water remain unfrozen as the pores of the soil are
 61 sufficiently small that ice cannot invade; the soil acts like a semi-permeable membrane
 62 and stops the ice from entering the soil pores (Gibbs-Thompson effect, cf Section 2.2).
 63 This is illustrated schematically in figure 2(b) which shows a close-up of the ice-lens soil
 64 interface. Due to the overlying weight, the pressure of ice in the lens is P_o (assumed
 65 isotropic [14]). Then equation (1) gives the water pressure necessary for equilibrium to
 66 be

$$P_{cl} = P_o - \frac{\rho_w L_f}{T_m} (T_m - T), \quad (2)$$

67 which we shall call the *Clapeyron pressure*.

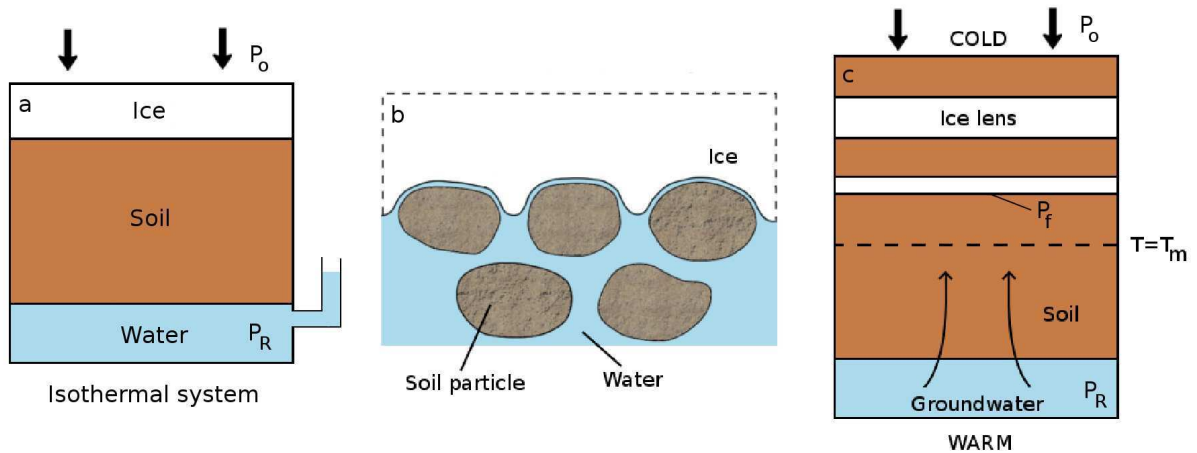


Figure 2: Schematic diagrams for the frost heave process. (a) A simple isothermal model of frost heave. (b) Microscopic view of the soil particles at the ice-soil interface. (c) A typical column of soil with multiple ice lenses. The soil is being frozen from the top down.

68 Suppose we initially fix the reservoir pressure $P_R = P_{cl}$ so the system is at equilibrium
 69 with no flow in the soil. If the temperature is reduced and P_o held constant, then equation
 70 (2) shows that P_{cl} decreases. If P_R is held constant, there will be a pressure drop across
 71 the soil layer and water will flow from the reservoir toward the ice lens, where it will freeze
 72 onto the lens, causing it to grow. Experimental realizations of this system demonstrate
 73 that if the reservoir has a sufficient supply of water at P_R , the ice lens can grow indefinitely,
 74 *heaving up* the surface [15, 16, 17]. The experiments also confirm that the flow can be
 75 stopped by either reducing the reservoir pressure, or increasing the overburden pressure
 76 P_o , until the equilibrium condition $P_R = P_{cl}$ is satisfied [15, 16, 17]. This water flow,
 77 and the associated accumulation of extra ice at the freezing front represents the basic
 78 capillary theory explanation of frost heave.

79 The Clapeyron equation explains thermodynamically why lowering the temperature
 80 below freezing in figure 2(a) causes water to be sucked towards an ice front. In order
 81 for the ice lens to grow, however, it is necessary for water to attach to ice at the ice-
 82 lens/soil boundary. A conceptual difficulty arises when we consider the interface between
 83 the soil and the ice lens, as shown in figure 2(b). If the soil particles are frozen to the ice,
 84 then the only place that water can attach to ice is along the pore space between the soil
 85 particles, and this will not result in a thickening ice lens. A resolution to this problem
 86 was conjectured by Taber [5, 6]. He suggested that microscopically-thin films of water
 87 exist between the ice and soil particle surfaces, and these allow water to flow around the

88 soil particles and attach evenly to the growing ice lens. As later work has shown, these
 89 ‘premelted’ films do exist, and are caused by molecular interactions between soil particles
 90 and ice [18, 19].

91 **2.2 Ice entry and the maximum frost heave pressure**

92 A key assumption of the capillary theory is that ice does not immediately penetrate
 93 into the pores of the soil as the temperature drops below T_m . This is a result of the
 94 Young-Laplace equation for the pressure difference across a curved ice-water interface
 95 [20]

$$P_i - P_w = \frac{2\gamma_{iw}}{r}, \quad (3)$$

96 where γ_{iw} is the ice-water surface energy and r is the radius of ice (assumed to approximate
 97 a spherical cap) adjacent to a pore. This is shown schematically in figure 2(b). If r is
 98 larger than the effective pore radius r_p , the ice cannot penetrate through the pore; ice
 99 can only invade once the pressure difference $\Delta P = P_i - P_w$ becomes sufficiently large
 100 that $r = r_p$. Thus ice invades the soil pores at the critical pressure difference

$$\Delta P_{max} = \frac{2\gamma_{iw}}{r_p}. \quad (4)$$

101 The temperature T_p at which ice invades the pores is found by combining (1) and (4) to
 102 obtain a form of the Gibbs-Thomson equation

$$T_p = T_m \left(1 - \frac{2\gamma_{iw}}{\rho_w L_f r_p} \right). \quad (5)$$

103 In the capillary model frost heave stops once $T \leq T_p$, when ice is assumed to fill the soil
 104 pores, blocking them and preventing water being sucked up to the growing lens. This
 105 gives rise to a *maximum frost-heave pressure*, P_m , which is the largest ice pressure that
 106 can occur before pore entry. If we note that the liquid pressure in the water column will
 107 always be $\leq P_R$ during freezing, then we can obtain P_m by combining equations (3) and
 108 (4) to give

$$P_m = P_R + \frac{2\gamma_{iw}}{r_p}. \quad (6)$$

109 The ideas expressed by equations (1)–(6) were tested extensively by early researchers
 110 and showed good quantitative agreement with experiments for monodisperse soils at
 111 temperatures close to T_m [21, 22, 23, 24, 25, 15, 26, 16, 27]. The simple isothermal
 112 capillary model can in principle be adapted to general soil-freezing situations such as that

113 shown in figure 2(c). A drop in air temperature causes freezing of the soil and ice lens
 114 formation. At the leading edge of the warmest ice lens the pressure drops – as discussed
 115 above – and this causes water to be sucked up from warm ($T > T_m$) groundwater to swell
 116 the lens, and heave the soil surface upwards. However, attempts to extend the capillary
 117 model to non-equilibrium situations led to some problematic shortcomings, as we discuss
 118 in the next section.

119 **2.3 Problems with the capillary theory**

120 Despite the ability of the capillary theory to explain the basic heaving phenomenon,
 121 significant deficiencies of the model became apparent in the 1960s and 1970s. Three
 122 major difficulties were identified by frost heave researchers.

123 **1) P_m predictions deviated from experiments in polydisperse soils.**

124 Predictions of the maximum frost-heave pressure matched well with experiments on
 125 idealized soils composed of monodisperse particles [22, 23]. However when soils containing
 126 a range of particle sizes were used, it was found that equation (6) did not agree with
 127 experimental results, as significantly larger heaving pressures were observed than were
 128 predicted [28, 29, 30].

129 **2) Break down of Clapeyron equation outside equilibrium.** Capillary theory can
 130 in principle be used to predict the flow rate towards the lens as the soil is frozen: for
 131 a rigid soil with homogeneous pore size Darcy’s law [31, 32] determines the flow rate
 132 towards the ice lens as

$$V = \frac{k}{\mu} \frac{P_R - P_f}{z_h}, \quad (7)$$

133 where k is the permeability of the soil, μ is the dynamic viscosity of water, and z_h is
 134 the distance between the ice lens and the reservoir of warm water. P_f is the pressure of
 135 the water directly below the warmest lens. Capillary theory assumes local equilibrium
 136 at the ice lens–soil boundary so that P_f is given by the Clapeyron equation (2), and
 137 with this assumption equation (7) determines V . However at rates typical of frost-heave
 138 experiments the equation tends to overpredict measured values of V by as much as several
 139 orders of magnitude [15, 16, 33, 32].

140 **3) No mechanism for initiation of new lenses.** A significant feature of frost heave
 141 is the sudden appearance of a new lens a finite distance below a previously growing lens,
 142 leading to a rhythmic banding structure such as shown schematically in figure 2(c). No

143 plausible mechanism within the capillary theory was offered to explain why ice lenses
144 form such discrete bands [34].

145 In Section 4 we review experimental and theoretical work demonstrating that these
146 obstacles to the capillary theory have been largely resolved, leading to an improved
147 capillary model. However, the difficulties seemed insurmountable in the 1970s and led
148 to the development of a radically different approach – the *frozen-fringe* model of frost
149 heave.

150 3 Frozen fringe models

151 The apparent failure of the capillary theory led some researchers [35, 36] to propose that
152 frost heave can continue to occur at ice-lens temperatures below T_p , *i.e.* after ice has
153 formed a *frozen fringe* by growing into the pores of the soil (figure 3). This assumption was
154 supported by experiments and modelling that demonstrated the existence of premelted
155 films at temperatures below T_p , thus potentially allowing slow transport of water through
156 the partially frozen region of the soil [37, 19]. The driving force causing flow in the fringe,
157 while initially uncertain, was eventually shown to be caused by thermomolecular pressure
158 gradients in the premelted films [38, 39]. An elegant demonstration of this process was
159 provided by Wilen and Dash [40], who developed a simple experimental analogue of a
160 frozen fringe using a capillary, and measured the flow in the premelted films. Theoretical
161 modelling using lubrication theory yielded very good agreement with the experimental
162 results [41, 42].

163 Harlan [36] was the first to propose equations for heat and matter flow in a frozen
164 fringe. His conservation of energy equation accounting for the phase change of unfrozen
165 water to ice took the form

$$\rho_s c_{ps} \frac{\partial T}{\partial t} = \frac{\partial}{\partial z} \left(k_s \frac{\partial T}{\partial z} \right) + \rho_i L_f \frac{\partial \phi_i}{\partial t}, \quad (8)$$

166 where ρ_s , c_{ps} and k_s are the density, specific heat capacity and thermal conductivity of the
167 partially frozen soil, and ϕ_i is the volume fraction of ice in the pore space, related to the
168 volume fraction of unfrozen water ϕ_w and soil particles ϕ_p by the identity $\phi_i + \phi_w + \phi_p = 1$.
169 In physical terms, this energy equation can be thought of as a diffusion equation for heat
170 in the frozen fringe, with an added source term due to latent heat release as the liquid
171 fraction freezes. To model mass transport Harlan [36] assumed Darcy’s law applies in

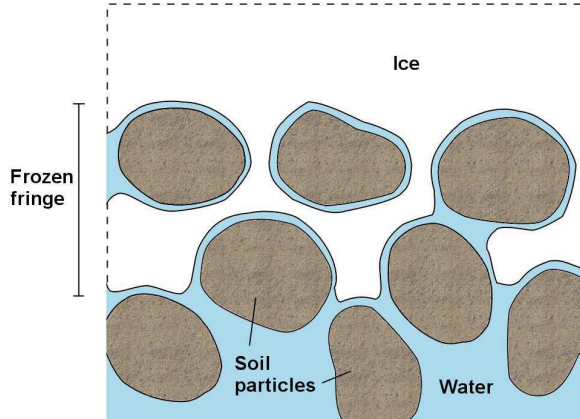


Figure 3: Schematic diagram of a freezing soil with a frozen fringe

172 the fringe, with an effective permeability that is a function of the water fraction ϕ_w .
 173 Although Harlan's equations did not permit the formation of discrete lenses, his theory
 174 provided a structure upon which subsequent researchers were able to propose conditions
 175 for new lenses.

176 The frozen-fringe hypothesis provided a potential resolution to the problems described
 177 in Section 2.3. Firstly, the suggestion that an ice lens can continue to grow after the ice
 178 invades the pore space means that there is no longer the constraint (6) on the maximum
 179 frost-heave pressure, allowing for larger values of P_m . Secondly, partial blocking of the
 180 pores of the soil in the frozen fringe causes slower flow of water towards a growing lens,
 181 and thus slower heave rates, potentially resolving the second difficulty with capillary
 182 theory. Finally, the existence of ice ahead of the growing lens provides nuclei from which
 183 new lenses can form and allows mechanisms to be advanced for the initiation of new
 184 lenses. For example, Miller [35, 34, 43, 44] built on the Harlan model by proposing an
 185 equation

$$\sigma_n = \sigma + (1 - \chi)P_i + \chi P_w, \quad (9)$$

186 to determine the effective stress σ_n acting on particles in the frozen fringe. Here $\sigma = -P_o$
 187 is the total stress and χ is a semi-empirical stress partition function that describes how the
 188 overlying weight is distributed between the pore ice and pore water in the frozen fringe.
 189 This function was introduced based on a similar stress partition function developed for
 190 unsaturated soil mechanics [45, 34]. Using Harlan's model to determine the temperature
 191 and fluid pressure in the fringe, Miller [34, 43] estimated the ice pressure using the
 192 Clapeyron equation and used this to keep track of σ_n . He found that, under certain

193 conditions, the effective stress between soil particles becomes positive – so the particles
194 in the soil can in principle separate – and proposed that a new ice lens would form at
195 this point.

196 Miller’s theory, which he referred to as secondary frost heaving (with capillary theory
197 referred to as primary heaving), was the first to yield quantitative predictions of lens
198 spacings. The frozen fringe concept has formed the basis of a large number of subsequent
199 theories [46, 47, 48, 49, 50, 51, 52, 53, 54, 55, 56, 57, 58, 59, 60, 61, 62, 63, 39, 64].
200 These works propose different physical explanations for the flow of premelted water in
201 the frozen fringe [39], as well as various mechanisms to characterize the stress state leading
202 to different ice-lens initiation criteria [46, 54, 56, 39]. There has also been substantial
203 work to provide simpler numerical solutions of the complex transport equations in the
204 frozen fringe. For example, Gilpin [46] proposed a somewhat simpler model than Miller’s,
205 in which new ice lenses form when the calculated ice pressure in the frozen fringe reaches
206 a critical separation pressure. Fowler [54] simplified the mathematics of the Miller model
207 by assuming the fringe thickness is asymptotically small. His theory allows for two
208 dimensional effects, potentially explaining differential frost heave and patterned ground
209 [57, 65]. Rempel et al. [39, 66] generalized models of flow in premelted films [41, 42] to
210 derive an expression for fluid transport in the frozen fringe. By performing a force balance
211 on particles in the fringe the model distinguishes parameter regimes for the growth of a
212 single lens, growth of multiple lenses to form a banded sequence, and freezing of the pore
213 space with no ice lenses.

214 As an example of the predictions of frozen-fringe models, figure 4 shows how different
215 frost-heave behaviours occur depending on the applied freezing conditions for represen-
216 tative soil parameters [39]. The diagram plots a nondimensional freezing velocity versus
217 a nondimensional overburden pressure, with G being the temperature gradient in the
218 sample. There are three main regimes that occur as the soil initially freezes: Firstly, in
219 the light grey region (at low V and P_o) a single ice lens will grow in a stable manner,
220 pushing all the soil particles ahead of it. Secondly, at higher freezing speeds in the white
221 region, periodic ice lenses form. Thirdly, when P_o is sufficiently large (dark grey region),
222 no heave can occur and so no ice lenses form. Rempel et al. [39] also noted that hys-
223 teresis is predicted near the regime boundaries (dashed lines). For instance, if the soil
224 is initially frozen in the periodic lens regime, and the freezing rate is dropped, the soil
225 will not revert to the steady lens behaviour until the conditions move below the bottom

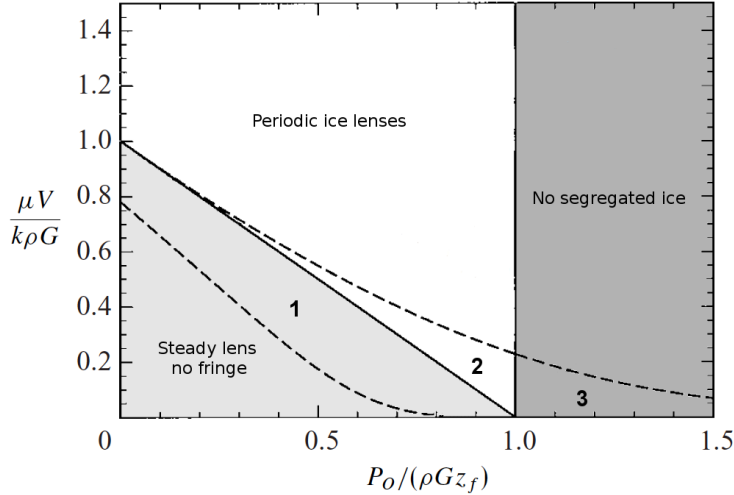


Figure 4: Regime diagram for soil freezing behaviour at different freezing speeds and overburden pressures, modified from Rempel et al. [39]. The behaviour in the different regimes is described in the text.

226 dashed line. Thus the behaviour in regimes 1 and 2 can be either a steady single lens
 227 or periodic ice lensing. Similarly in regime 3, there can either be no segregated ice, or a
 228 steady single lens.

229 Results such as those in figure 4 show that frozen fringe models can replicate many of
 230 the qualitative changes in behaviour that are seen in experiments. Frozen fringe models
 231 have also had some success at making quantitative predictions of heave rates [46, 58,
 232 67], though detailed comparisons with experiment have proven challenging [68]. Further
 233 details regarding the capillary and frozen-fringe models can be found in review articles
 234 by Rempel [69], Dash et al. [19], Black [68], Smith [70] and O’Neill [71].

235 3.1 Does the frozen fringe exist?

236 A key question distinguishing the capillary and secondary heave models is whether ice
 237 lenses form within a frozen fringe, or whether they always grow without entering the pore
 238 space. Despite a substantial amount of experimental work, this has proven difficult to
 239 answer. The pore size in typical frost-heaving soils is on the order of $1\mu\text{m}$ in diameter, and
 240 so pore-scale effects are difficult to probe directly. Furthermore, the indices of refraction
 241 of water and ice are very close to each other which means that it is not possible to
 242 distinguish optically when pore ice appears, unlike the process of soil desaturation [72].

243 Thus many experiments have resorted to indirect estimation of when a frozen fringe has
244 occurred, for instance by estimating when the temperature drops below T_p [73, 74].

245 That ice lenses can form in a frozen fringe is perhaps best demonstrated by their
246 appearance in rocks. In this case the migration of freezing water into large pores or
247 microcracks of the rock pushes open the cracks, leading to fracturing of the rock and the
248 formation of new lenses [75, 76]. It has been shown that the pressures that act to force
249 open new cracks are only sufficiently large to fracture the rock when the temperature
250 drops well below the pore freezing temperature of the rock [74]. In this case it seems
251 likely that water is drawn through a frozen-fringe-like region of rock to feed the growing
252 ice lenses.

253 Other evidence for frozen fringes are not so clear cut. For instance, one of the main
254 experiments supporting the frozen-fringe hypothesis in silty soils was published by Loch &
255 Kay [73]. They measured the temperature of ice-lens formation in New Hampshire silt and
256 found that it was colder than their estimation of the pore freezing temperature T_p . This
257 appears to be evidence supporting the existence of a frozen fringe. However, Loch & Kay
258 did not take account of the polydispersity of the soil, known to have significant impacts
259 on T_p [11, 30]. If we use the expression of Everett [11] for the ice-entry temperature of a
260 polydisperse soil to recalculate T_p for Loch & Kay's experiment then the results are less
261 certain (see Section 4).

262 To further complicate matters there is an increasing amount of experimental data
263 showing that in soils composed of clay and fine silt sized particles, ice lenses can indeed
264 form without a frozen fringe. For example, Beskow [7] stressed repeatedly that in clays
265 and fine silts the soil between the warmest ice lenses is unfrozen:

266 The very important fact that in an ice-banded frozen soil with a moderately
267 low temperature, the soil between the ice bands is fully plastic and soft,
268 therefore unfrozen, has not been considered... In fine clays, cooled only a few
269 degrees below freezing, all the pore water is unfrozen, leaving the clay between
270 the ice layers plastic and soft...

271 he goes on to say

272 Near the frost line (where the temperature is only slightly below 0 °C) the soil
273 between the ice layers is unfrozen and soft even in silty soils.... [In clays] not
274 only near the frost line, but also higher up, the soil is just as soft and plastic

275 as it is under this level. Thus in clays at moderately low temperatures, the
276 soil itself between the ice layers is soft and unfrozen.

277 Brown [77] placed blocks of saturated soil on a thin layer of ice and then slowly reduced
278 the temperature of the system. He found that, during sufficiently slow freezing, water
279 from the soil would flow to the ice, causing it to thicken while the soil consolidated. At
280 a critical temperature the soil block stopped shrinking and upon examination was solid
281 and frozen. Brown concluded that ice had entered the pores and defined this critical
282 temperature as the pore freezing temperature T_p . The value for T_p was later confirmed
283 via differential scanning calorimetry experiments [78]. Importantly, Brown [77] noticed
284 that if the temperature was reduced too quickly, ice lenses formed in the interior of the
285 block of soil. These ice lenses always formed at temperatures warmer than T_p , consistent
286 with the capillary theory and contradicting the frozen-fringe hypothesis (which requires
287 ice lenses to form at temperatures colder than T_p).

288 Akagawa [79] measured the thermal conductivity of frozen soil, anticipating that the
289 thermal properties of frozen soil would be distinct from those of unfrozen soil. As expected
290 Akagawa [79] found that the thermal conductivity of regions of soil containing ice lenses
291 was higher than that of the unfrozen soil. In contrast, in the region between the warmest
292 ice lens and the 0°C isotherm (where the frozen fringe was expected to be located) the
293 measured thermal conductivity was indistinguishable from that of the unfrozen soil [79].

294 Takeda and Okamura [80] and Watanabe et al. [81] used light microscopy to examine
295 under high magnification the soil adjacent to the warmest ice lens in freezing samples
296 of Kanto loam and Fujinomori clay. They found no evidence of ice in the frozen fringe
297 region, and no significant structural changes that might be expected if ice were forming
298 in the pores of the soil. In one experiment, Takeda and Okamura [80] followed a large
299 fluid-filled pore as it migrated into the frozen fringe region. If the fringe contained ice,
300 it was expected that water in the large pore would freeze. However, the water remained
301 unfrozen until the pore was broken by a crack-shaped ice lens.

302 Finally, Watanabe and Mizoguchi [82] devised an improved version of the Loch and
303 Kay [73] experiment. They developed a novel Raman-spectroscopy technique capable of
304 detecting pore ice. In a setup similar to Loch and Kay's, and using a soil composed of
305 fine, silt-sized particles ($10\ \mu\text{m}$ diameter), Watanabe and Mizoguchi [82] found that no
306 pore ice was present in the soil ahead of the growing ice lens. As a result they concluded
307 that frozen fringe theories are not applicable to their system.

308 As a result of conflicting experimental results, it does not seem possible at the present
309 time to conclusively say whether or not frozen fringes exist. Indeed it is likely that a frozen
310 fringe may be present in some systems and not in others, with its presence depending
311 upon the soil material and the rate of freezing. Importantly though, on the basis of the
312 evidence above, we can conclude that in some systems a sequence of ice lenses can form
313 without the presence of a frozen fringe. This suggests that there must be a mechanism
314 by which new ice lenses can form within the framework of the capillary theory. In the
315 next section we describe recent work that has revived the capillary theory by proposing
316 new mechanisms for the initiation of ice lenses and potentially resolving the objections
317 raised in Section 2.3.

318 4 Revised capillary theory

319 With recent experimental work seeming to conclusively demonstrate ice-lens formation
320 without a frozen fringe in some systems, frost heave researchers have been led to readdress
321 the problems with capillary theory. Here we show that the major objections to the
322 capillary model listed in Section 2.3 can be resolved via a combination of early neglected
323 explanations and more recent results.

324 **1) P_m predictions deviated from experiments in polydisperse soils.** As discussed
325 in Section 2.3, the capillary theory accurately predicts the maximum heaving pressures
326 in monodisperse soils, but gives smaller pressures than observed in tests on soils with a
327 broad particle-size distribution. It can be shown, however, that an error is introduced
328 if the effective pore size is estimated based on air-entry measurements. Studies have
329 shown that air entry values are determined by the largest pore sizes in a sample, which
330 in turn are determined by the largest particle sizes in the sample [83]. As an example, in
331 the experiments of Loch and Kay [73] discussed in Section 3.1, a pore size of $8\ \mu\text{m}$ was
332 obtained from air-entry measurements, corresponding to the largest 10% of particles in
333 their sample.

334 In contrast to the air-entry process, when ice grows next to a soil surface a sorting
335 process occurs, reducing the effective pore size of the soil. That is, the largest particles
336 in a sample tend to be engulfed by an ice interface while smaller particles are pushed
337 ahead [84, 85, 86]. Thus a boundary layer of relatively small particles will tend to form
338 against a growing ice lens, with the inter-particle pore size being significantly reduced.

339 This means that the pore size at ice entry can be significantly smaller than the pore size
340 at air entry.

341 If we accept assertions that the ice-entry pressure is determined by the smallest par-
342 ticles in a soil due to the mechanism above [11, 30], the apparent contradictions with
343 capillary theory appear to be resolvable. For example, Sutherland and Gaskin [30] show
344 that good agreement with equation (3) is obtained if Everett’s [11] proposal that T_p is
345 determined by the smallest 10% of particles is used to determine maximum pressures.
346 Experiments capable of monitoring particle size and rearrangements at the surface of a
347 growing ice lens will help to further clarify this issue.

348 **2) Failure of Clapeyron equation outside equilibrium.** Even in soils composed of
349 uniform particles, the Clapeyron equation (1) was observed to break down at significant
350 freezing rates (as opposed to equilibrium measurements taken after ice lenses stopped
351 growing, when the equation works well) [15, 16, 33]. A first explanation for this was
352 proposed by Jackson et al. [10] who demonstrated that viscous flow in premelted films
353 between an ice lens and soil particles becomes important at finite freezing rates. Similar
354 ideas were presented by several subsequent authors [18, 87, 88, 89, 90, 91, 92, 32]. As
355 demonstrated by Style and Peppin [32], accounting for the viscous resistance to flow in
356 the films shows that the Darcy pore pressure at the ice lens P_f (c.f. figure 2(c)) is given
357 by a generalized Clapeyron equation containing a kinetic term:

$$P_f = P_o - \frac{\rho_w L_f}{T_m} (T_m - T) + V f(T_m - T), \quad (10)$$

358 where V is the growth rate of the ice lens and f is a function of temperature that can be
359 measured or calculated from the geometry of the soil particles. The Clapeyron equation
360 (2) is recovered when the growth rate is small, however the additional term in equation
361 (10) causes the flow rate to the growing ice lens to be significantly reduced in typical
362 freezing scenarios. Using (10) with Darcy’s law (7), predicted flow rates can be matched
363 with experimental measurements [32].

364 Equation (10) also quantifies the dependence of frost heave on particle size. For soils
365 made up of larger particles, the viscous resistance effect results in a large reduction in
366 flow rate, as typically $f(T_m - T)$ is proportional to the square of the particle size [32]. On
367 the other hand, for soils consisting of smaller particles the flow rate is reduced because of
368 the low permeability of the soil. Thus there is a maximum heave rate for soils composed
369 of intermediate-sized particles. This is seen in experiments, where frost-susceptibility is

370 known to be greatest for medium-grained soils such as silts [7]. Equation (10) can in
371 principle predict the optimum particle size for soil of a given material [32].

372 **3) Mechanism for initiation of new lenses.** As discussed in Section 2.3, a major
373 drawback of the capillary theory was its failure to explain how ice lenses form in discrete
374 bands. Beskow [7] and Martin [93] suggested that the region in front of a growing ice
375 lens would become progressively supercooled, allowing a new ice lens to nucleate in a
376 flaw or large pore. Beskow [7] further noted the resemblance of ice lens growth to a
377 fracture process, and hypothesized that supercooling ahead of a growing ice lens may
378 provide a source of energy for a new lens to nucleate. However, these ideas were not
379 quantified or explored further. Nevertheless, recent work has shown that the basic ideas
380 have merit, with two main potential mechanisms for fringe-free ice-lens formation having
381 been proposed.

382 **4.1 Fringe-free models of intermittent lensing**

383 **4.1.1 Engulfment model**

384 Mutou et al. [94] performed a series of experiments where they froze a dilute suspension
385 of soil particles in a cell. They did this by imposing a fixed temperature gradient on the
386 cell, and then pulling the cell at a fixed rate, so that freezing occurred at a constant speed.
387 For pulling speeds in excess of a critical velocity V_c all the particles were engulfed by the
388 ice front, while for speeds below V_c the particles were pushed ahead by the ice – just as
389 single particles are rejected ahead of a growing ice lens at low freezing speeds [85, 86].
390 At speeds just below V_c , Mutou et al. [94] observed that a layer of particles would build
391 up against the ice interface and then suddenly become engulfed when the layer reached
392 a certain thickness. Repetition of this process yielded a banded structure which partially
393 resembled a sequence of ice lenses. Watanabe et al. [95] explained the engulfment of
394 the layer as owing to the viscous drag of the particle layer (in addition to the drag of
395 the premelted films at the ice–particle layer interface) which reduces the effective critical
396 velocity required for engulfment. They hypothesized that a similar process occurs during
397 ice lens formation in soils [95]. That is, a compacted region of particles builds up against
398 the warm face of a growing ice lens. Once the compacted region reaches a certain critical
399 thickness the ice interface engulfs the compacted layer and a new lens forms at a less
400 consolidated region of soil. A similar explanation was proposed by Jackson et al. [10]

401 and Zhu et al. [96].

402 The engulfment model is a viable mechanism for the formation of ice bands. Whether
403 such bands are the same thing as ice lenses is an open question, with recent experiments
404 suggesting bands form at much higher freezing velocities than ice lenses [97, 98]. In
405 addition the model of Watanabe et al. [95] requires the soil between ice lenses to be
406 frozen and hence cannot explain some observations of clays and fine silts that show the
407 soil between the warmest ice lenses to be unfrozen [7, 77]. A useful test of the theory
408 would therefore be to use a technique such as that of Watanabe & Mizoguchi’s [82] to
409 search for pore ice in the soil on the cold side of a growing ice lens.

410 4.1.2 Geometrical supercooling model

411 In order to gain insight into observations of fringe-free ice lens formation, Peppin et al.
412 [99] developed a Stefan model of the growth of a single ice lens adjacent to a saturated
413 soil composed of rigid spherical particles. The model finds that the soil adjacent to an ice
414 lens consolidates and at fast freezing rates can become constitutionally supercooled. This
415 constitutional supercooling is entirely analogous to the constitutional supercooling that is
416 found in solidifying alloys and freezing aqueous solutions [100]. Later work demonstrated
417 that, in non-cohesive soils and colloidal suspensions, when constitutional supercooling
418 occurs the ice/soil interface is morphologically unstable [101, 102]. The instability results
419 in dendritic ice structures which grow rapidly into the freezing suspension [101]. This
420 model provides a thermodynamic explanation for the presence of supercooling and seg-
421 regated ice in otherwise unfrozen soil, though gives little information on the structure
422 and orientation of the ice. Extensions of this work led to a “mushy layer” model of
423 frost heave [103] analogous to mushy layer models of dendritic ice in alloys [104]. Similar
424 mixed-phase models were proposed by Arakawa [105] and Chalmers and Jackson [106].
425 Peppin et al. [103] and Chalmers and Jackson [106] found using this model that the rate
426 of heave is independent of the rate of soil freezing, in agreement with experimental results
427 of Beskow [7], Ueda and Penner [107] and Watanabe [33].

428 Style et al. [14] extended the constitutional supercooling concept to cohesive soils that
429 may or may not contain pore ice and referred to the phenomenon in general as *geometrical*
430 *supercooling*. They extended the single ice-lens model [99] to look at the anisotropic stress
431 state that develops in a cohesive soil next to a growing ice lens. Motivated by observations
432 which showed that the opening of a new ice lens appears to be a fracture process [7, 99],

433 they considered the growth of an ice-filled flaw in the supercooled region ahead of a
 434 growing lens. When the ice pressure in the flaw reaches a critical pressure $P_i = P_o + \sigma_t$
 435 it overcomes the tensile strength of the soil σ_t and the overlying weight P_o . This allows
 436 the flaw to crack open across the soil forming a new lens. The critical condition can be
 437 rewritten as

$$T_{cl} - T = \Delta T_c \quad (11)$$

438 where T_{cl} is the *Clapeyron temperature*, that is, the temperature at which a new ice lens
 439 can exist stably at equilibrium, and $\Delta T_c = T_m \sigma_t / (\rho_w L_f)$. For a soil with pore pressure
 440 profile $P_w(z, t)$ and overburden P_o , the Clapeyron temperature is determined from (1) as

$$T_{cl}(z, t) = T_m \left(1 - \frac{P_o - P_w(z, t)}{\rho_w L_f} \right). \quad (12)$$

When the gradient in Clapeyron temperature at the ice lens surface is larger than the
 temperature gradient, ie when

$$\frac{\partial T_{cl}}{\partial z} > \frac{\partial T}{\partial z},$$

441 the soil ahead of the lens is geometrically supercooled. A representative profile of T and
 442 T_{cl} is shown schematically in figure 5. The maximum geometrical supercooling occurs at
 443 a finite distance ahead of the growing lens, and when this maximum reaches ΔT_c , a new
 444 ice lens can form. As shown in section 4, the temperature at the surface of the ice lens is
 445 given by equation (10) as $T = T_{cl} - V/\kappa_u$, where $\kappa_u = \rho_w L_f / [T_m f(T_m - T)]$ is a kinetic
 446 supercooling coefficient. Figure 5 illustrates the case considered by Style et al. [14] when
 447 κ_u is large and the kinetic term is small.

448 Style et al. [14] showed that geometrical supercooling will occur when there is a
 449 significant drop in the permeability of the soil directly ahead of the growing ice lens.
 450 They suggested three possible causes: the formation of a frozen fringe, desaturation
 451 of the soil, and compaction of a compressible soil. Each of these is known to occur,
 452 and will certainly provide enough supercooling to allow periodic ice lenses to grow [14].
 453 Importantly the latter two mechanisms do not require a frozen fringe to be present.

454 An obvious difficulty is how an ice-filled crack appears ahead of an ice lens if there
 455 is no frozen fringe. Style et al. [14] conclude, as did Scherer [108], that spontaneous
 456 nucleation of ice in pores is not likely. Instead they suggest that new lenses can nucleate
 457 from the side of ice-filled shrinkage cracks that are known to extend some distance ahead
 458 of the warmest ice lens [7, 109, 110]. This is shown schematically in figure 6(a), while
 459 figure 6(b) shows shrinkage cracks protruding ahead of an ice lens in a typical freezing soil

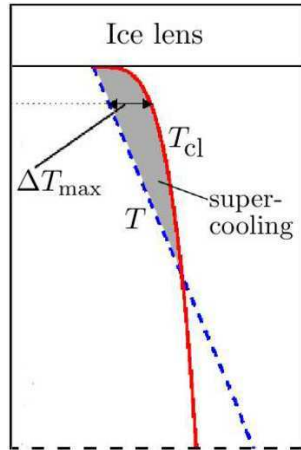


Figure 5: Schematic diagram showing geometrical supercooling in a freezing soil. A maximum in the supercooling exists at a finite distance ahead of the growing ice lens. A new lens will form at this point when the supercooling reaches the ΔT_c .

460 [110]. Ice lens formation in this manner would result in ladder-like patterns of segregated
 461 ice, and this is indeed seen in many experiments [7, 109, 101, 110], with a typical example
 462 in figure 7. Alternatively new lenses may nucleate off pre-existing lenses as cracks which
 463 curve down to form a new lens, resulting in a different morphology which is also seen in
 464 frost heave experiments [5, 6].

465 This theory shows very good qualitative agreement with experimental observations.
 466 Quantitatively, the model agrees with measurements of the temperature at which new
 467 ice lenses form in two experimental systems [14], and work is currently ongoing to test
 468 predictions of lens spacings and lens thicknesses against additional experiments. Fur-
 469 ther application of the principles and procedures of fracture mechanics may be useful in
 470 determining the key parameters are that control ice-lens patterns during freezing.

471 5 Discussion

472 As will have become apparent, there are still many questions that must be answered in
 473 order to give a complete picture of the physics of frost heave. Several experimental issues
 474 that present themselves are:

- 475 • Under what conditions does frozen-fringe/fringe-free formation of periodic lenses
 476 occur?

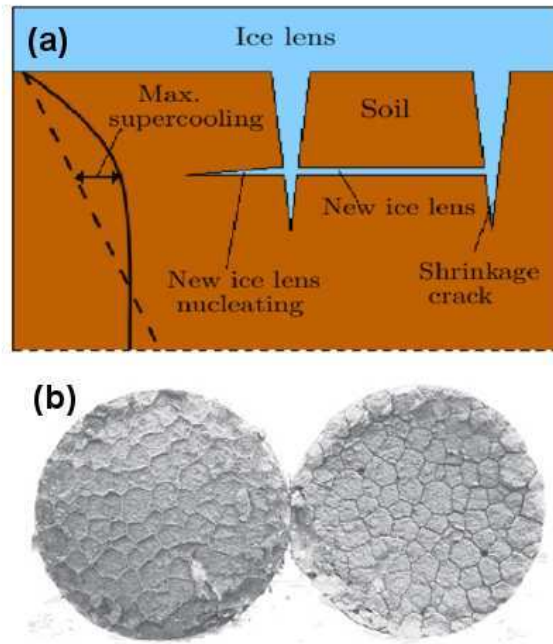


Figure 6: (a) Schematic diagram showing how new ice lenses can nucleate off the side of shrinkage cracks that grow into the soil ahead of an existing ice lens. (b) A freezing block of Devon silt that is broken open at the freezing front [110]. The left hand block is the upper, frozen soil. The right hand block is the warmer, unfrozen soil. A polygonal network of shrinkage cracks can clearly be seen extending out of the frozen material. The sample diameter is about 100mm.

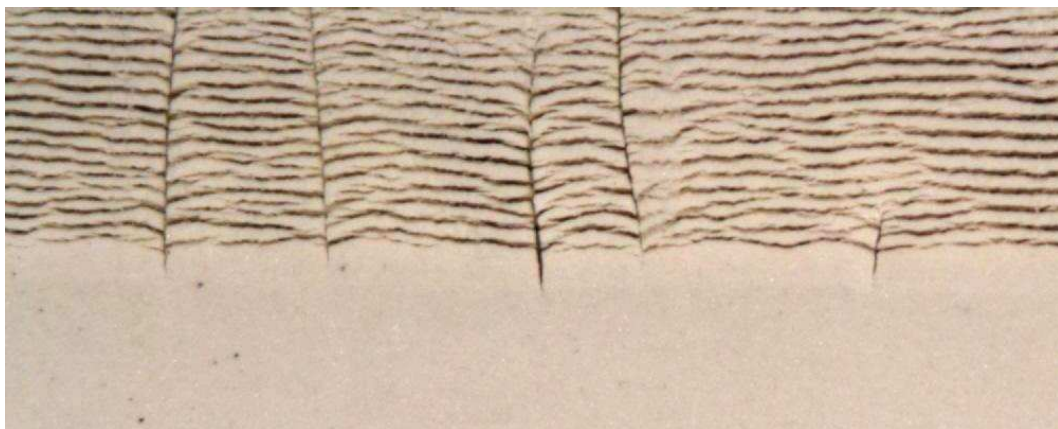


Figure 7: Ice lenses forming in a freezing sample of kaolinite. The clay is frozen in the directional solidification of Peppin et al. [102]. Image height is approximately 2 cm. Vertical shrinkage cracks can clearly be seen, giving the ladder-like structure discussed in the text.

- 477 • Can the same type of soil exhibit periodic lensing with and without a frozen fringe?
- 478 • If both frozen-fringe and fringe-free lensing occur, is one mode more dangerous than
479 the other? We might expect fringe-free heave rates to be faster due to the lack of
480 pore-blocking by ice.
- 481 • Can the engulfment model of ice lenses be verified by looking for pore ice behind
482 newly formed ice lenses?

483 At the same time, there is still a substantial amount of theoretical work to be done. One
484 of the key reasons for understanding frost heave is to be able to understand soil movement
485 for geophysical and engineering applications, and so it is important to be able to extend
486 the models above into three dimensions. Both theoretical and experimental work are also
487 needed to explore further aspects of frost heave that have not been captured above. For
488 instance

- 489 • How is frost heave affected by the presence of solutes in the pore water [111], soil
490 cohesiveness, polydispersity [11, 30] and unsaturated conditions [112]?
- 491 • How do ice-filled cracks propagate through a soil? What controls their horizontal
492 growth rate? Can they be modelled with unfrozen soil parameters?
- 493 • Can frost heave models be extended to two and three dimensions and used to explain
494 the formation of patterned ground [65]? Can such models of patterned ground be
495 used to give insight on past climate conditions [113, 1]?

496 The fact that so many questions remain demonstrates that, despite its long history,
497 there is still much work to be done to understand frost heave and its effects. However,
498 with the recent progress made using new experimental and theoretical techniques, this is
499 certainly an exciting time to be involved in the field. We hope that this review serves to
500 stimulate new research that can advance the field, and unlock many of the puzzles that
501 remain.

502 **6 Conclusion**

503 In this review we have discussed the various mathematical models that have been pro-
504 posed to explain frost heave and the growth of ice lenses in freezing soils. While early

505 theories based on the capillary model captured many of the essential features and showed
506 good agreement with experiment, deficiencies of the model including its underprediction
507 of frost heave pressures and its failure to explain the rhythmic banding of ice lenses led
508 many researchers to abandon it in favour of a fundamentally distinct secondary frost
509 heave model. The secondary heave model allows ice lenses to form within a partially
510 frozen fringe, in contrast to the capillary theory which only permits ice lenses to grow at
511 the freezing front. Experimental work is divided over the issue: in some systems a frozen
512 fringe appears to be present, while in others it is absent. The latter observations have
513 motivated a revisit of the capillary theory, and recent work shows that its previous defi-
514 ciencies have been substantially resolved, albeit with the theory in a significantly revised
515 form. The particle-engulfment and the geometrical supercooling models are summarized
516 yielding new mechanisms for the periodic formation of ice lenses that are consistent with
517 capillary theory. Some open problems are also discussed. It is hoped the review will
518 stimulate experimental and theoretical developments leading to further insight into an
519 intriguing geophysical phenomenon.

520 **7 Acknowledgements**

521 This publication is based on work supported by Award No. KUK-C1-013-04, made by
522 King Abdullah University of Science and Technology (KAUST). RWS is funded by a Yale
523 University Bateman Interdepartmental Postdoctoral Fellowship.

524 **References**

- 525 [1] C. Gallagher, M.R. Balme, S.J. Conway, and P.M. Grindrod. Sorted clastic stripes, lobes
526 and associated gullies in high-latitude craters on mars: Landforms indicative of very
527 recent, polycyclic ground-ice thaw and liquid flows. *Icarus*, 211:458–471, 2011.
- 528 [2] A. DiMillio. *A Quarter Century of Geotechnical Research*. Federal Highway Administra-
529 tion, Washington, DC, 1999.
- 530 [3] A. C. Palmer and P. J. Williams. Frost heave and pipeline upheaval buckling. *Canadian*
531 *Geotechnical Journal*, 40:1033–1038, 2003.
- 532 [4] S. Taber. The growth of crystals under external pressure. *American Journal of Science*,
533 37:532–556, 1916.

- 534 [5] S. Taber. Frost heaving. *J. Geol.*, 34:428, 1929.
- 535 [6] S. Taber. The mechanics of frost heaving. *Journal of Geology*, 38:303–317, 1930.
- 536 [7] G. Beskow. *The Swedish Geological Society, C, no. 375, Year Book no. 3*. Technological
537 Institute, Northwestern University, 1935. Reprinted in *Historical Perspectives in Frost*
538 *Heave Research* (P. B. Black and M. J. Hardenberg, eds.) CRREL Special Report No.
539 91-23, pp 37–157, 1991.
- 540 [8] L. W. Gold. A possible force mechanism associated with the freezing of water in porous
541 materials. *Highway Research Board Bulletin*, 168:65–72, 1957.
- 542 [9] K. Jackson and B. Chalmers. Freezing liquids in porous media with reference to frost
543 heaving in soils. *Journal of Applied Physics*, 29:1178–1181, 1958.
- 544 [10] K. A. Jackson, D. R. Uhlmann, and B. Chalmers. Frost heave in soils. *Journal of Applied*
545 *Physics*, 37:848–852, 1966.
- 546 [11] D. H. Everett. The thermodynamics of frost damage to porous solids. *Transactions of*
547 *the Faraday Society*, 57:1541–1551, 1961.
- 548 [12] I. Prigogine and R. Defay. *Chemical Thermodynamics*. Longmans Green and Co., London,
549 1954.
- 550 [13] P. B. Black. *Applications of the Clapeyron equation to ice and water in porous media*,
551 pages 1–7. CRREL Special Report No. 95-6. 1995.
- 552 [14] R. W. Style, S. S. L. Peppin, A. C. F. Cocks, and J. S. Wettlaufer. Ice lens formation
553 and geometrical supercooling in soils and other colloidal materials. *Physical Review E*,
554 84:041402, 2011.
- 555 [15] F. J. Radd and D. H. Oertle. Experimental pressure studies of frost heave mechanisms
556 and the growth-fusion behaviour of ice. In *2nd International Conference on Permafrost*,
557 pages 122–129, Yakutsk, 1960.
- 558 [16] M. B. G. M. Biermans, K. M. Dijkema, and D. A. De Vries. Water movement in porous
559 media towards an ice front. *Journal of Hydrology*, 37:137–148, 1978.
- 560 [17] H. Ozawa and S. Kinoshita. Segregated ice growth on a microporous filter. *Journal of*
561 *Colloid and Interface Science*, 132:113–124, 1989.
- 562 [18] B. V. Derjaguin and N. V. Churaev. The theory of frost heaving. *Journal of Colloid and*
563 *Interface Science*, 67:391–396, 1978.

- 564 [19] J. G. Dash, A. W. Rempel, and J. S. Wettlaufer. The physics of premelted ice and its
565 geophysical consequences. *Rev. Mod. Phys.*, 78:695–741, 2006.
- 566 [20] R. Defay and I. Prigogine. *Surface Tension and Adsorption*. Longmans, London, 1966.
- 567 [21] E. Penner. The mechanism of frost heaving in soils. *Highway Research Board Bulletin*,
568 225:1–13, 1959.
- 569 [22] E. Penner. Pressures developed in a porous granular system as a result of ice segregation.
570 *Highway Research Board Special Report*, 40:191–199, 1959.
- 571 [23] R. D. Miller, J. H. Baker, and J. H. Kolaian. Particle size, overburden pressure, pore water
572 pressure and freezing temperature of ice lenses in soils. In *7th International Congress of*
573 *Soil Scientists, Transactions*, volume 1, pages 122–129, 1960.
- 574 [24] E. Penner. Pressures developed during the unidirectional freezing of water-saturated
575 porous materials. In *Proceedings of the International Conference on Low Temperature*
576 *Science*, volume 1, pages 1401–1412, Sapporo, Japan, 1967.
- 577 [25] E. Penner. Frost heaving pressures in particulate materials. In *Organisation for Economic*
578 *Co-Operation and Development Symposium on Frost Action on Roads*, volume 1, pages
579 379–385, Paris, France, 1973.
- 580 [26] M. Vignes and K. M. Dijkema. A model for the freezing of water in a dispersed medium.
581 *Journal of Colloid and Interface Science*, 49:165–172, 1974.
- 582 [27] E. Penner and L. E. Goodrich. Location of segregated ice in frost-susceptible soil. *Engi-*
583 *neering Geology*, 18:231–244, 1981.
- 584 [28] E. Penner. Heaving pressure in soils during unidirectional freezing. *Canadian Geotechnical*
585 *Journal*, 4:398–408, 1967.
- 586 [29] J.P.G. Loch and R. D. Miller. Tests of the concept of secondary heaving. *Soil Science*
587 *Society of America Proceedings*, 39:1036–1041, 1975.
- 588 [30] H. B. Sutherland and P. N. Gaskin. Pore water and heaving pressures developed in
589 partially frozen soils. In *2nd International Conference on Permafrost*, volume 1, pages
590 409–419, Yakutsk, 1973.
- 591 [31] M. K. Hubbert. *The Theory of Ground Water Motion*. Hafner Publishing Co., NY, 1969.
- 592 [32] R. W. Style and S. S. L. Peppin. The kinetics of ice-lens growth in porous media. *Journal*
593 *of Fluid Mechanics*, 692:482–498, 2012.

- 594 [33] K. Watanabe. Relationship between growth rate and supercooling in the formation of ice
595 lenses in a glass powder. *J. Cryst. Growth*, 237:2194–2198, 2002.
- 596 [34] R. D. Miller. Lens initiation in secondary heaving. In *Proceedings of the International*
597 *Symposium on Frost Action in Soils*, volume 2, pages 68–74, 1977.
- 598 [35] R.D. Miller. Freezing and heaving of saturated and unsaturated soils. *Highway Research*
599 *Record*, 393:1–11, 1972.
- 600 [36] R. L. Harlan. Analysis of coupled heat-fluid transport in partially frozen soil. *Water*
601 *Resources Research*, 9:1314–1323, 1973.
- 602 [37] J. W. Cahn, J. G. Dash, and H.-Y. Fu. Theory of ice premelting in monosized powders.
603 *J. Cryst. Growth*, 123:101–108, 1992.
- 604 [38] J. G. Dash. Thermomolecular pressure in surface melting: a motivation for frost heave.
605 *Science*, 246:1591, 1989.
- 606 [39] A. W. Rempel, J. S. Wettlaufer, and M. G. Worster. Premelting dynamics in a continuum
607 model of frost heave. *J. Fluid Mech.*, 498:227–244, 2004.
- 608 [40] L. A. Wilen and J. G. Dash. Frost heave dynamics at a single crystal interface. *Physical*
609 *Review Letters*, 74:5076–5079, 1995.
- 610 [41] J. W. Wettlaufer and M. G. Worster. The dynamics of premelted films: Frost heave at a
611 capillary. *Physical Review E*, 51:4679–4689, 1995.
- 612 [42] J. S. Wettlaufer and M. G. Worster. Premelting dynamics. *Ann. Rev. Fluid Mech.*,
613 38:427–452, 2006.
- 614 [43] R. D. Miller. Frost heaving in non-colloidal soils. In *Proceedings of the 3rd International*
615 *Conference on Permafrost*, volume 1, pages 708–713, 1978.
- 616 [44] K. O’Neill and R. D. Miller. Exploration of a rigid ice model of frost heave. *Water*
617 *Resources Research*, 21:281–296, 1985.
- 618 [45] A. W. Bishop and G. E. Blight. Some aspects of effective stress in saturated and partially
619 saturated soils. *Geotechnique*, 13:177–197, 1963.
- 620 [46] R. R. Gilpin. A model for the prediction of ice lensing and frost heave in soils. *Water*
621 *Resources Research*, 16:918–930, 1980.

- 622 [47] S. W. Hopke. A model for frost heave including overburden. *Cold Regions Science and*
623 *Technology*, 3:177–183, 1980.
- 624 [48] J. M. Konrad and N. R. Morgenstern. A mechanistic theory of ice lens formation in
625 fine-grained soils. *Canadian Geotechnical Journal*, 17:473–486, 1980.
- 626 [49] S. Takagi. The adsorption force theory of frost heaving. *Cold Regions Science and Tech-*
627 *nology*, 1:57–81, 1980.
- 628 [50] T. V. Hromadka, G. L. Guymon, and R. L. Berg. Some approaches to modeling phase
629 change in freezing soils. *Cold Regions Science and Technology*, 4:137–145, 1981.
- 630 [51] M. Fremond, H. Ghidouche, and N. Point. Freezing of a porous medium with water supply
631 coupled stefan problem. *Journal of Mathematical Analysis and Applications*, 108:371–402,
632 1985.
- 633 [52] J. Walder and B. Hallet. A theoretical model of the fracture of rock during freezing.
634 *Geological Society of America Bulletin*, 96:336–346, 1985.
- 635 [53] K. Horiguchi. An osmotic model for soil freezing. *Cold Regions Science and Technology*,
636 14:13–22, 1987.
- 637 [54] A. Fowler. Secondary frost heaving in freezing soils. *SIAM Journal on Applied Mathe-*
638 *matics*, 49:991–1008, 1989.
- 639 [55] Y. Nakano. Quasi-steady problems in freezing soils: I. analysis on the steady growth of
640 an ice layer. *Cold Regions Science and Technology*, 17:207–226, 1990.
- 641 [56] J. F. Nixon. Discrete ice lens theory for frost heave in soils. *Canadian Geotechnical*
642 *Journal*, 28:843–859, 1991.
- 643 [57] A. Fowler and W. B. Krantz. A generalized secondary frost heave model. *SIAM Journal*
644 *on Applied Mathematics*, 54:1650–1675, 1993.
- 645 [58] J. M. Konrad and C. Duquennoi. A model for water transport and ice lensing in freezing
646 soils. *Water Resources Research*, 29:3109–3124, 1993.
- 647 [59] R. L. Michalowski. A constitutive model of saturated soils for frost heave simulations.
648 *Cold Regions Science and Technology*, 22:47–63, 1993.
- 649 [60] L. Bronfenbrener and E. Korin. Kinetic model for crystallization in porous media. *Inter-*
650 *national Journal of Heat and Mass Transfer*, 40:1053–1059, 1997.

- 651 [61] N. Li, F. Chen, B. Su, and G. Cheng. Theoretical frame of the saturated freezing soil.
652 *Cold Regions Science and Technology*, 35:73–80, 2002.
- 653 [62] A. Y. Sheshukov and A. G. Egorov. Frozen barrier evolution in saturated porous media.
654 *Advances in Water Resources*, 25:591–599, 2002.
- 655 [63] F. Talamucci. Freezing processes in porous media: Formation of ice lenses, swelling of the
656 soil. *Mathematical and Computer Modelling*, 37:595–602, 2003.
- 657 [64] H. R. Thomas, P. Cleall, Y.-C. Li, C. Harris, and M. Kern-Leutschg. Modelling of cryo-
658 genic processes in permafrost and seasonally frozen soils. *Geotechnique*, 59:173–184, 2009.
- 659 [65] R. A. Peterson and W. B. Krantz. A mechanism for differential frost heave and its
660 implications for patterned-ground formation. *Journal of Glaciology*, 49:69–80, 2003.
- 661 [66] A. W. Rempel. Formation of ice lenses and frost heave. *J. Geophys. Res.*, 112:F02S21,
662 2007.
- 663 [67] L. Bronfenbrener and R. Bronfenbrener. Modeling frost heave in freezing soils. *Cold*
664 *Regions Science and Technology*, 61:43–64, 2010.
- 665 [68] P. B. Black. *Historical perspective of frost heave research*, pages 1–7. CRREL Special
666 Report No. 91-23. 1991.
- 667 [69] A. W. Rempel. Frost heave. *Journal of Glaciology*, 56:1122–1128, 2010.
- 668 [70] M. W. Smith. *Models of soil freezing*, pages 96–120. Field and Theory: Lectures in
669 Geocryology. University of British Columbia Press, Vancouver, 1985.
- 670 [71] K. O’Neill and R. D. Miller. The physics of mathematical frost heave models: A review.
671 *Cold Regions Science and Technology*, 6:275–291, 1983.
- 672 [72] L. Xu, S. Davies, A. B. Schofield, and D. A. Weitz. Dynamics of drying in 3d porous
673 media. *Physical Review Letters*, 101:094502, 2008.
- 674 [73] J.P.G. Loch and B. D. Kay. Water redistribution in partially frozen, saturated silt under
675 several temperature gradients and overburden loads. *Soil Science Society of America*
676 *Journal*, 42:400–406, 1978.
- 677 [74] B. Hallet, J. S. Walder, and C. W. Stubbs. Weathering by segregation ice growth in
678 microcracks at sustained sub- zero temperatures: Verification from an experimental study
679 using acoustic emissions. *Permafrost and Periglacial Processes*, 2:283–300, 1991.

- 680 [75] J. Walder and B. Hallet. A theoretical model of the fracture of rock during freezing.
681 *Geological Society of America Bulletin*, 96:336–346, 1985.
- 682 [76] I. Vlahou and M. G. Worster. Ice growth in a spherical cavity of a porous medium.
683 *Journal of Glaciology*, 56:271–277, 2010.
- 684 [77] S. C. Brown. *Soil Freezing*. PhD thesis, University of Reading, Reading, UK, 1984.
- 685 [78] S. C. Brown and D. Payne. Frost action in clay soils. ii. ice and water location and suction
686 of unfrozen water in clays below 0 °c. *Journal of Soil Science*, 41:547–561, 1990.
- 687 [79] S. Akagawa. Experimental study of frozen fringe characteristics. *Cold Regions Science
688 and Technology*, 15:209–223, 1988.
- 689 [80] K. Takeda and A. Okamura. *Microstructure of freezing front in freezing soils*. Ground
690 Freezing 97. Balkema, Rotterdam.
- 691 [81] K. Watanabe, M. Mizoguchi, T. Ishizaki, and M. Fukuda. *Experimental study on mi-
692 crostructure near freezing front during soil freezing*. Ground Freezing 97. Balkema, Rot-
693 terdam.
- 694 [82] K. Watanabe and M. Mizoguchi. Ice configuration near a growing ice lens in a freezing
695 porous medium consisting of micro glass particles. *J. Cryst. Growth*, 213:135–140, 2000.
- 696 [83] D. Hillel. *Introduction to Environmental Soil Physics*. Elsevier, USA, 2004.
- 697 [84] A. E. Corte. Particle sorting by repeated freezing and thawing. *Science*, 142:499–501,
698 1963.
- 699 [85] D. R. Uhlmann, B. Chalmers, and K. A. Jackson. Interaction between particles and a
700 solid/liquid interface. *J. Appl. Phys.*, 35:2986–2992, 1964.
- 701 [86] A. W. Rempel and M. G. Worster. The interaction between a particle and an advancing
702 solidification front. *J. Cryst. Growth*, 205:427–440, 1999.
- 703 [87] T. Forland and S. K. Ratkje. Irreversible thermodynamic treatment of frost heave. *En-
704 gineering Geology*, 18:225–229, 1981.
- 705 [88] B. V. Derjaguin and N. V. Churaev. Flow of nonfreezing water interlayers and frost
706 heaving. *Cold Regions Science and Technology*, 12:57–66, 1986.
- 707 [89] T. Kuroda. Role of water layer at an ice surface in the kinetic processes of growth of ice
708 crystals. *Journal de Physique*, 48:487–493, 1987.

- 709 [90] T. Tsuneto. Remarks on frost heave. *Journal of the Physical Society of Japan*, 63:2231–
710 2234, 1994.
- 711 [91] M. G. Worster and J. S. Wettlaufer. *The Fluid Mechanics of Premelted Liquid Films*,
712 pages 339–351. Fluid Dynamics at Interfaces. Cambridge University Press, Cambridge,
713 UK, 1999.
- 714 [92] A. W. Rempel. A theory for ice-till interactions and sediment entrainment beneath
715 glaciers. *J. Geophys. Res.*, 113:F01013, 2008.
- 716 [93] R. T. Martin. Rythmic ice banding in soil. *Highway Research Board Bulletin*, 218:11–23,
717 1959.
- 718 [94] Y. Mutou, K. Watanabe, M. Mizoguchi, and T. Ishizaki. Microscopic observation of ice
719 lensing and frost heaves in glass beads. In *Proceedings of the 7th International Conference*
720 *on Permafrost*, pages 783–787, Yellowknife, Canada, 1998.
- 721 [95] K. Watanabe, Y. Muto, and M. Mizoguchi. A model for the formation of ice lenses in an
722 unconfined, water-saturated porous medium consisting of spherical particles. In *Ground*
723 *Freezing 2000. Frost Action in Soils: Proceedings of the 9th International Symposium*,
724 pages 55–60, Louvain-La-Neuve, Belgium, 2000.
- 725 [96] D.-M. Zhu, O. E. Vilches, J. G. Dash, B. Sing, and J. S. Wettlaufer. Frost heave in argon.
726 *Physical Review Letters*, 85:4908–4911, 2000.
- 727 [97] S. Deville, E. Maire, G. Bernard-Granger, A. Lasalle, A. Bogner, C. Gauthier, J. Leloup,
728 and C. Guizard. Metastable and unstable cellular solidification of colloidal suspensions.
729 *Nature Mat.*, 8:966–972, 2009.
- 730 [98] A. Lasalle, C. Guizard E. Maire, J. Adrien, and S. Deville. Particle redistribution and
731 structural defect development during ice templating. *Acta Materiala*, page in press, 2012.
- 732 [99] S. S. L. Peppin, J. A. W. Elliott, and M. G. Worster. Solidification of colloidal suspensions.
733 *J. Fluid Mech.*, 554:147–166, 2006.
- 734 [100] S. H. Davis. *Theory of Solidification*. Cambridge University Press, UK, 2001.
- 735 [101] S. S. L. Peppin, M. G. Worster, and J. S. Wettlaufer. Morphological instability in freezing
736 colloidal suspensions. *Proc. Roy. Soc. Lond. A*, 463:723–733, 2007.
- 737 [102] S. S. L. Peppin, J. S. Wettlaufer, and M. G. Worster. Experimental verification of morpho-
738 logical instability in freezing aqueous colloidal suspensions. *Phys. Rev. Lett.*, 100:238301,
739 2008.

- 740 [103] S. S. L. Peppin, A. Majumdar, R. W. Style, and G. J. Sander. Frost heave in colloidal
741 soils. *SIAM Journal on Applied Mathematics*, 71:1717–1732, 2011.
- 742 [104] M. G. Worster. *Solidification of fluids*, pages 393–446. Perspectives in Fluid Dynamics.
743 Cambridge University Press, Cambridge, UK, 2000.
- 744 [105] K. Arakawa. Theoretical studies of ice segregation in soil. *Journal of Glaciology*, 6:255–
745 260, 1966.
- 746 [106] B. Chalmers and K. A. Jackson. Experimental and theoretical studies of the mechanism
747 of frost heaving. *CRREL Research Report*, 199:1–22, 1970.
- 748 [107] T. Ueda and E. Penner. Mechanical analogy of a constant heave rate. In *Proceedings of*
749 *the International Symposium on Frost Action in Soils*, pages 57–67, Sweden, 1978.
- 750 [108] G. W. Scherer. Freezing gels. *Journal of Non-Crystalline solids*, 155:11–25, 1993.
- 751 [109] E. J. Chamberlain and A. J. Gow. Effect of freezing and thawing on the permeability and
752 structure of soils. *Engineering Geology*, 13:73–92, 1979.
- 753 [110] L. U. Arenson, T. F. Azmatch, and D. C. Sego. A new hypothesis on ice lens formation
754 in frost-susceptible soils. In *9th International Conference on Permafrost*, volume 1, pages
755 59–64, Alaska, 2008.
- 756 [111] K. Watanabe, Y. Muto, and M. Mizoguchi. Water and solute distributions near an ice lens
757 in a glass-powder medium saturated with sodium chloride solution under unidirectional
758 freezing. *Crystal Growth & Design*, 1:207–211, 2001.
- 759 [112] S. A. Shoop and S. R. Bigl. Moisture migration during freeze and thaw of unsaturated
760 soils: modeling and large scale experiments. *Cold Regions Science and Technology*, 25:33–
761 45, 1997.
- 762 [113] A. Kade and D. A. Walker. Experimental alteration of vegetation on nonsorted circles:
763 Effects on cryogenic activity and implications for climate change in the arctic. *Arctic,*
764 *Antarctic, and Alpine Research*, 40:96–103, 2008.

RECENT REPORTS

12/11	Parasite spill-back from domestic hosts may induce an Allee effect in wildlife hosts	Krkošek Ashander Lewis
12/12	Modelling temperature-dependent larval development and subsequent demographic Allee effects in adult populations of the alpine butterfly <i>Parnassius smintheus</i>	Wheeler Bampfylde Lewis
12/13	Putting “space” back into spatial ecology	Fortin Peres-Neto Lewis
12/14	Wildlife disease elimination and density dependence	Potapova Merrill Lewis
12/15	Spreading Speed, Traveling Waves, and Minimal Domain Size in Impulsive Reaction-diffusion Models	Lewis Li
12/16	MCMC methods for functions modifying old algorithms to make them faster	Cotter Roberts Stuart White
12/17	Weyl Geometry and the Nonlinear Mechanics of Distributed Point Defects	Yavari Goriely
12/18	A note on oblique water entry	Moore Howison Ockendon Oliver
12/19	Calculus on surfaces with general closest point functions	März Macdonald
12/20	Multiple equilibria in a simple elastocapillary system	Taroni Vella
12/21	Multiphase modelling of vascular tumour growth in two spatial dimensions	Hubbard Byrne
12/22	Chebfun and Numerical Quadrature	Hale Trefethen
12/23	Moment-based formulation of NavierMaxwell slip boundary conditions for lattice Boltzmann simulations of rarefied flows in microchannels	Reis Dellar
12/24	Correspondence between one- and two-equation models for solute transport in two-region heterogeneous porous media	Davit Wood Debenest Quintard

12/25	Rolie-Poly fluid flowing through constrictions: Two distinct instabilities	Reis Wilson
12/26	Age related changes in speed and mechanism of adult skeletal muscle stem cell migration	Collins-Hooper Woolley Dyson Patel Potter Baker Gaffney Maini Dash Patel
12/27	The interplay between tissue growth and scaffold degradation in engineered tissue constructs	ODEa Osborne El Haj Byrne Waters
12/28	Non-linear effects on Turing patterns: time oscillations and chaos.	Aragon Barrio Woolley Baker Maini
12/29	Colorectal Cancer Through Simulation and Experiment	Kershaw Byrne Gavaghan Osborne
12/30	A theoretical investigation of the effect of proliferation and adhesion on monoclonal conversion in the colonic crypt	Miramis Fletcher Maini Byrne
12/31	Convergent evolution of spiny mollusk shells points to elastic energy minimum	Chirat Moulton Shipman Goriely
12/32	Three-dimensional oblique water-entry problems at small dead-rise angles	Moore Howison Ockendon Oliver
12/33	Second weak order explicit stabilized methods for stiff stochastic differential equations	Abdulle Vilmart Zygalakis
12/34	The sensitivity of Graphene 'Snap-through' to substrate geometry	Wagner Vella

Copies of these, and any other OCCAM reports can be obtained from:

**Oxford Centre for Collaborative Applied Mathematics
Mathematical Institute
24 - 29 St Giles'
Oxford
OX1 3LB
England**

www.maths.ox.ac.uk/occam